Published in *Supercond. Sci. Technol.* (*SuST*) **23**, 034017 (2010)

Ac losses in non-inductive coated conductor coils with field-dependent critical current density

Francesco Grilli[1], Frédéric Sirois[2], Simon Brault[2], Roberto Brambilla[3], Luciano Martini[3], Doan N. Nguyen[4] and Wilfried Goldacker[1]

[1] Forschungszentrum Karlsruhe GmbH, Hermann-von-Helmholtz-Platz 1, D-76344 Eggenstein-Leopoldshafen, Germany

[2] Ecole Polytechnique de Montréal, PO Box 6079 Station Centre-ville, Montréal QC, H3C 3A7 Canada

[3] ENEA - Ricerca sul Sistema Elettrico S.p.A., Via Rubattino 54, I-20134 Milano, Italy

[4] Los Alamos National Laboratory, Los Alamos, NM 87545, USA

E-mail: `francesco.grilli@kit.edu`

Abstract. In this paper we consider two different finite-element models for computing ac losses in coils composed of coated conductors: a 2-D model based on solving Maxwell equations by means of edge elements and a 1-D model based on solving the integral equations for the sheet current density in the tapes. The models are tested for a configuration of practical interest, a non-inductive solenoidal coil for fault current limiter applications. We focused our attention on the conditions when differences between the two models are expected to emerge, for example when the tapes are closely packed together or where the dependence of the critical current density on the local magnetic field is taken into account. We present and discuss several cases, offering possible explanations for the observed differences of ac loss values.

1. Introduction

Finite-element method have proved to be a powerful tool for computing ac losses in high-temperature superconductor (HTS) tapes and assemblies [1]. The choice of the model to be utilized for designing low loss devices may depend on several factors, including accuracy and computation speed. Recently, we have focused our attention on a 1-D approach to simulate second-generation HTS tapes: being much faster than standard 2-D models, it can be attractive for optimizing the design of HTS device, when a large number to simulations has to be carried out, in order to investigate the influence of the various parameters. Whereas the 1-D model, which by its nature cannot consider the variation of electromagnetic quantities across the tape's thickness, has proved to provide identical results to those of the 2-D model in the case of an isolated tape, it has still to be investigated if this good agreement is preserved in situations when the interaction between neighboring tapes is particularly strong, e.g. when they are closely packed together.

In this paper, we compare the 1-D and the 2-D models in the case of a non-inductive "tape arrangement", focusing on the situations where difference between the two models start to appear and on their causes. The geometry of a non-inductive solenoid can be utilized for fault current limiter applications [2, 3]. It is characterized by closely packed, electromagnetically interacting tapes, and it is therefore ideal to investigate the differences between the two models.

2. Geometry and numerical models

We consider the internal part of the solenoid corresponding to most of the tape turns, where the end effects do not play an important role. This allows us to focus on the difference between the two models. A schematic view of the geometry is given in figure 1, where the two superposed tapes (carrying opposite currents) are representative of each layer. Due to the symmetry of the geometry, only one 'periodic cell' needs to be simulated. L_x is the size of this periodic cell, which accounts for the width of the tape and the lateral gap between the turns. The inter-layer separation is given by L_z.

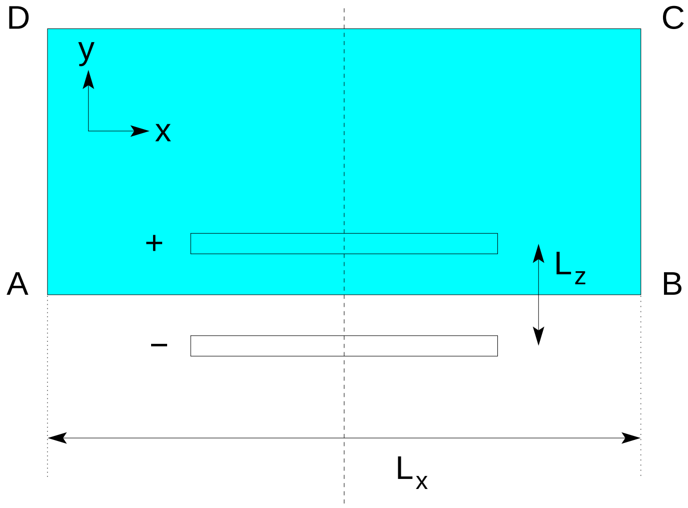

Figure 1. Cross-section of two superposed tapes representing the periodic cell of an anti-inductive solenoid. The colored area represents the area simulated in the 2-D model. On the AB, BC, and DA domain boundaries the Dirichlet condition H_y=0 is applied; on the CD boundary the Neumann condition is applied. The +/− signs indicate that the current flows in opposite direction in the two layers (in and out of the page). Not drawn to scale.

The utilized models have been described in two previous works of ours [4, 5]: the 2-D model solves Maxwell equations by means of edge elements; the 1-D model considers the coated conductor as infinitely thin and solves (by finite elements) the following integro-differential equation for finding the sheet current density $J(x,t)$:

$$\rho J(x,t) = \frac{\mu d}{2\pi} \int_{-a}^{a} \dot{J}(\xi,t) \left[\ln \sin \frac{\pi |x-\xi|}{L_x} - \frac{1}{2} \ln \left(\cosh \frac{2\pi L_z}{L_x} - \cos \frac{2\pi (x-\xi)}{L_x} \right) \right] \mathrm{d}\xi, \qquad (1)$$

where a is the half width of the tape, d its thickness and ρ is the electrical resistivity.

The 2-D model uses the magnetic field components as state variables. The geometry of the two-layer solenoid presents a symmetry plane that allows simulating only one tape in the cell. In figure 1 the colored area denotes the simulated geometry. In the considered case, the current flows in opposite direction in the two layers; this results in the condition H_y=0 along the AB boundary. Due to the lateral periodicity of the geometry the same conditions holds along the BC and DA boundaries. In the simulated geometry the Dirichlet boundary condition $H_y = 0$

is therefore set along the boundaries AB, BC, and DA. On the CD boundary, which is situated much farther from the tapes than represented in the figure, the tangential component of the field is left free to vary (Neumann condition). For the simulations, the problem can be further simplified by taking into account only one half of the tape and by applying the condition $H_y = 0$ on the dashed line displayed in figure 1. Even with all this simplification, the 2-D model is still quite time consuming: the computation time of one ac cycle with a mesh sufficiently fine to obtain smooth profiles is in the range 1,000-10,000 seconds[1], depending on the considered current amplitude and tape separation.

In the 1-D model the anti-inductive configuration is taken into account directly in the form of the integral equation for the current density – see [6] for details. With the 1-D model simulations are much faster, in the order of a few minutes.

In both models the superconductor is described by a non-linear resistivity, derived from a power-law $E(J)$ characteristic: $E = E_c(J/J_c)^n$. In this paper we considered the following values for the superconductor's parameters, which are typical of commercially available coated conductors: width $2a$=10 mm, I_c=300 A (self-field at 77 K), n=25. In the 2-D model the superconductor is simulated as 10 μm thick, in order to keep the number of nodes at a reasonable level. Since the minimum inter-layer separation considered in this paper is much higher (250 μm), this is a reasonable approximation.

3. Dependence of J_c on the magnetic field

Assuming a constant value for J_c in the $E(J)$ characteristic might be a strong approximation, since the dependence of J_c on the magnetic field exhibited by coated conductor tapes can affect their performance. This is particularly true in assemblies of HTS tapes (cables, coils, etc.), where each tape is subjected not only to its self-field, but also the the magnetic field generated by neighboring tapes. It is beyond the scope of this article to give a precise $J_c(B)$ characterization of coated conductors, since it inevitably depends on the quality of the sample, the manufacturing technique, and many other parameters. The important point is that for our models we need to input a $J_c(B)$ characteristic, where B is the vector representing the *local* magnetic field. How to derive a realistic $J_c(B)$ characteristic from experiments is a delicate issue, since usually one measures the reduction of the critical current I_c as a function of the *applied* field, from which deriving $J_c(B)$ is not trivial. A good approach is the following: (i) make some physical assumptions leading to a $J_c(B)$ function depending on a certain number of parameters; (ii) build a numerical model for the considered HTS tape; (iii) find the parameters of the $J_c(B)$ that optimize the $V - I$ characteristics with respect to the measured ones. This approach has been described in detail and successfully tested in [7] and [8], respectively. For our tests, we utilized a $J_c(B)$ model based on the results of Rostila *et al* [8]:

$$J_c(B_y) = J_{c0} \cdot \left[1 + \frac{|B_y|}{B_0}\right]^{-\alpha}, \qquad (2)$$

where B_y is the local magnetic field component perpendicular to the tape's face, B_0=25 mT, and α=0.75. Since we compared the 2-D model with the 1-D one, which by its nature cannot take into account the magnetic field component parallel to the tape's face, in our $J_c(B)$ model the dependence on the parallel component is omitted.

The implementation of the $J_c(B)$ relation (2) is quite different in our two models: in the 2-D model, the two components of the magnetic field are the state variables, so that the variable B_y is directly available during the computation. In the 1-D model, things are more complex, because the model used the sheet current density J as state variable, and B_y needs to be computed by means of the Biot-Savart law:

[1] On a workstation with a 2-GHz clock speed and 4 GB of RAM.

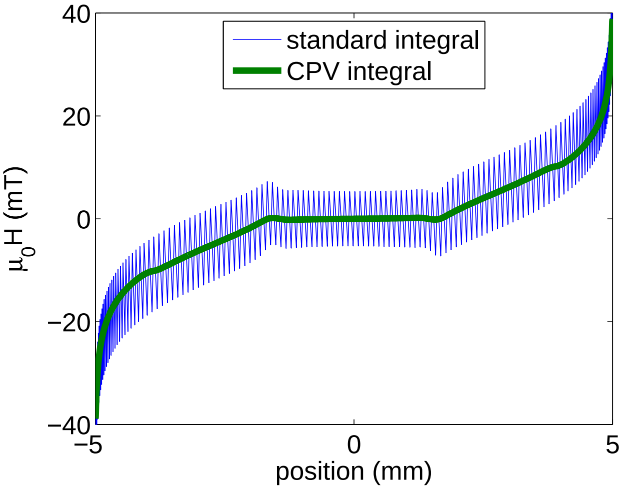

Figure 2. Magnetic field profile along the tape width computed with the standard and CPV integration. The transport current is $0.9I_c$.

$$B_y(x) = \frac{\mu_0}{2\pi}\int_{-a}^{a}\frac{J(\xi)}{\xi - x}\mathrm{d}\xi. \tag{3}$$

Due to the strong singularity of the integrand when $\xi = x$, this integral has to be considered in the sense of Cauchy Principal Value (CPV). This kind of integration is not available in the software package used for the model implementation [9]. Using the standard routines offered to the user results in large oscillations of the calculated magnetic field profile, as can be seen in figure 2. In order to overcome this obstacle, we define the CPV integral as follows:

$$B_y(x) = \Re\left[\frac{\mu_0}{2\pi}\int_{-a}^{a}\frac{J(\xi)}{\xi - x + i\epsilon}\mathrm{d}\xi\right], \tag{4}$$

where $i\epsilon$ is a small imaginary quantity inserted to remove the singularity. By this artifice the integral 4 is turned back into a normal integral. While lacking any mathematical rigor, this method was tested on many analytical examples and we found its results more than acceptable for our purpose.

The question is how small ϵ should be. It cannot be too small, because it would be ineffective. On the other hand, if it is too large it would affect significantly the computation of B_y. We found that the best choice is choosing ϵ of the same size of the mesh elements. This is easy to do in the case of a regular mesh. However, in our 1-D model we usually use a non-uniform mesh (coarser in the center of the tape and finer near the edges), in order to be able to investigate situations when the magnetic flux penetrates over a small distance from the edge, for example when the transport current is low. In our program, there is the possibility to set ϵ equal to the size of the local mesh element h, so that ϵ is automatically adapted to the different size of the mesh elements along the tape's width.

Figure 2 shows a typical field profile obtained with standard integration and CPV integration of equation (3).

4. Results

In this section, we present the results of our computations. First we compare the losses as a function of the transport current computed with the 2-D and 1-D model; then we discuss the effects of the use of a $J_c(B)$ relation in the two models; finally, we investigate the influence of the tape separation on the ac losses.

4.1. Comparison between 2-D and 1-D model

In our previous works we have already presented a comparison of the results obtained with the 2-D and 1-D models (both in the case of isolated and interacting tapes), obtaining very good agreement between the two models [5, 6]. The much shorter computation times of the 1-D model made it look as the preferable choice for performing simulations. It has to be noted, however, that the cases of interacting tapes presented in [6] were for relatively large tape separations. In this section we present a more detailed comparison between the two models, focusing on small tape separation, when differences between the models begin to emerge [10, 11].

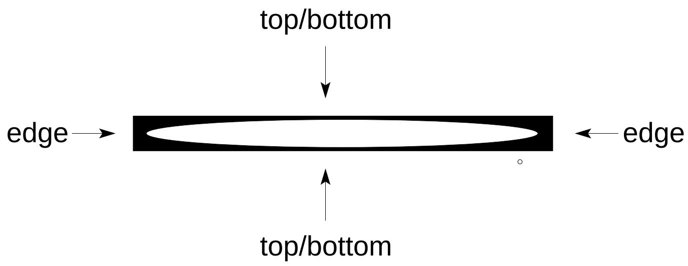

Figure 3. Schematic drawing of the regions where edge and top/bottom losses occur.

In a rectangular tape, the penetration of the magnetic flux (causing dissipation) can occur both from the edges of the tape and from the flat faces of the tape [10]. This is schematically represented in figure 3. In the case of an isolated thin tape, the first mechanism is dominant. When thin tapes are close and carry opposite current, the magnetic field flux lines are compressed in the space between the tapes and a substantial magnetic field parallel to the tape' face is created. This parallel magnetic field causes flux penetration in the superconductor from the top and bottom faces, which contributes to the total ac losses [11]. This contribution can become the main source of dissipation, depending on the tape separation and on the current carried by the tape. For sake of clarity, we call the two types of dissipation *edge* and *top/bottom* losses, respectively, as prposed by Clem [10].

The 1-D model, by its nature, can take into account only the edge losses. It is therefore interesting to see what are the limits of its applicability and what is the error done by neglecting the top/bottom losses.

Figure 4 displays the ac losses as a function of the transport current for different values of the inter-layer separation, computed with the two models. In figure 4(a), 4(b), and 4(c) the losses computed with the 2-D model are split into the edge and top-bottom components. The method used to separate the two loss components will be described soon in a forthcoming paper. First, it can be noted that the losses computed with the two models are generally different, and they become similar only at large separations, e.g. 5 mm – see figure 4(c). Second, the excellent agreement between the losses computed with the IE model and the edge losses computed with the 2-D model constitutes a good proof that the IE model only takes into account the edge losses." A similar sentence should be corrected in the conclusion. From figure 4(d) it can be observed that the losses computed with the IE model get closer to the total losses computed with the 2-D model at higher currents and larger separation. This can be explained as follows:

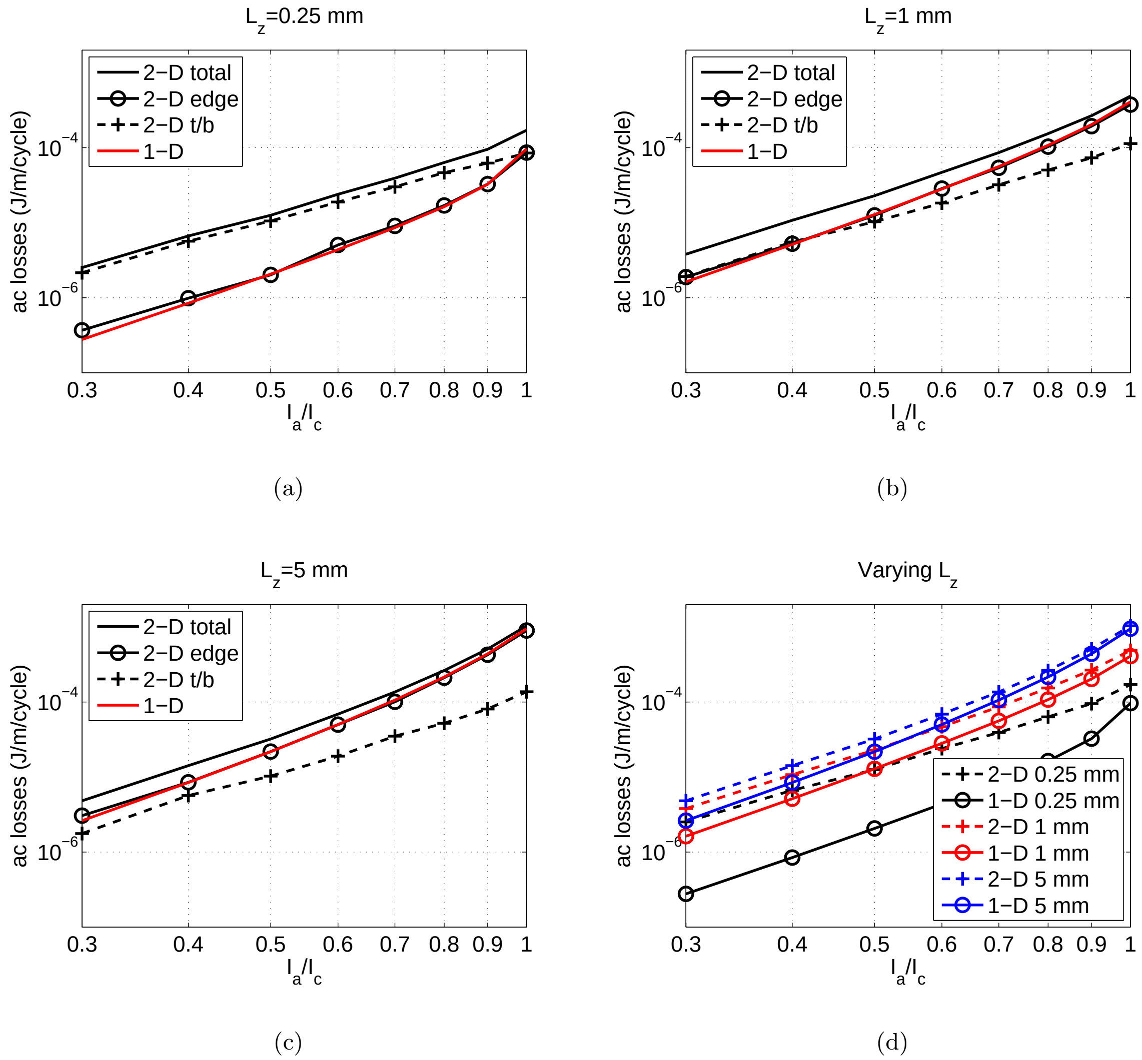

Figure 4. Ac losses as a function of the transport current for different values of the inter-layer separation, computed with the two models. In figures (a)-(c) the losses computed with the 2-D model are split in the contributions coming from the edge and top-bottom.

- At higher transport currents, the penetration of the magnetic flux from the edge becomes more important, so that the edge losses are predominant – see also [10].
- At larger inter-tape separation, the tapes are less influenced by the neighbors: again, the edge losses are predominant.

4.2. Losses with field-dependent J_c

As mentioned before, it is beyond the scope of this article to present a $J_c(B)$ relation that describes real YBCO CC samples and also compares the results obtained with constant and field-dependent J_c. In this section, we would like to investigate the effects of inserting a $J_c(B)$ characteristic used to model the superconductors. In particular, we investigate the consequences of using a $J_c(B)$ relation in the 2-D and 1-D model. In doing that, we use for J_{c0} in (2) the same value used in the model with constant J_c, which inevitably results in a lower *effective*

Table 1. Influence of the ϵ parameter in equation (4) on the ac losses (in J/m/cycle) for different values of the inter-layer separation L_z and of the applied transport current.

L_z / ϵ	0.25 mm h	1 mm h	5 mm h	0.25 mm $2h$	1 mm $2h$	5 mm $2h$	0.25 mm $h/2$	1 mm $h/2$	5 mm $h/2$
0.3	5.45E-07	3.20E-06	5.23E-06	5.08E-07	3.00E-06	4.96E-06	5.60E-07	3.28E-06	5.34E-06
0.4	1.89E-06	1.10E-05	1.89E-05	1.80E-06	1.05E-05	1.79E-05	1.94E-06	1.13E-05	1.92E-05
0.5	5.30E-06	3.10E-05	5.67E-05	5.00E-06	2.96E-05	5.28E-05	5.45E-06	3.19E-05	5.77E-05
0.6	1.34E-05	7.74E-05	1.52E-04	1.26E-05	7.31E-05	1.42E-04	1.37E-05	7.98E-05	1.58E-04
0.7	3.47E-05	1.87E-04	4.01E-04	3.20E-05	1.75E-04	3.68E-04	3.66E-05	1.93E-04	4.19E-04
0.8	1.25E-04	4.84E-04	1.13E-03	1.08E-04	4.42E-04	1.02E-03	1.34E-04	5.08E-04	1.18E-03
0.9	7.87E-04	1.73E-03	3.61E-03	6.91E-04	1.56E-03	3.30E-03	8.37E-04	1.80E-03	3.79E-03
1	1.29E-02	1.41E-02	1.74E-02	1.05E-02	1.18E-02	1.50E-02	1.43E-02	1.56E-02	1.88E-02

critical current of the tape. This means, for example, that when we apply a transport current I_a=0.8I_c (where I_c is the critical current for the constant-J_c case), we are actually applying a higher fraction of the real, effective critical current. But – once again – this is not a matter of concern, because we want to compare the influence of using a $J_c(B)$ relation in the 2-D and 1-D model and not compare the results obtained with constant-J_c and $J_c(B)$ models.

Firstly, we studied the influence of the ϵ parameter in equation (4) on the ac losses computed with the 1-D model. The results are summarized in table 1 for different values of the inter-layer separation L_z and of the applied transport current. We considered three values for ϵ: h, $2h$ and $h/2$, where h represents the size of the local mesh elements. The loss values are quite stable, and they are almost always within 10% of the value obtained with $\epsilon = h$. As mentioned before, considering larger value of h gives very different loss values, whereas considering smaller value does not solve the problem of the numerical oscillations in the magnetic field profiles.

Secondly, we compared the results with those obtained with the 2-D model. In general, we found that the results obtained with the two models are quite different, and for some values of the current and tape separations they are very different. As an example, figure 5 shows the ac losses as a function of the transport current for an inter-layer separation of 0.250 mm and 1 mm, respectively. It can be noticed that the 1-D results are far from the 2-D ones and that, contrary to the constant-J_c case, the losses computed with the 1-D model are also far from the edge loss contribution computed with the 2-D model.

The reason for this result is that, since the 1-D model can account only for the edge losses, it tends to 'amplify' the losses in the field dependent case. Indeed, since J_c is reduced, the edge penetration is increased much, whereas in the 2-D model, the finite tape thickness can somehow limit this penetration effect, especially because the field is not forced to be purely perpendicular across the whole tape width.

4.3. Losses as a function of the tape separation

We studied the influence of the distance between tapes, both horizontal (dimension of the periodic cell L_x) and vertical (layer separation L_z), using the 2-D model with $J_c(B)$ dependence. In general, we found that the inter-layer separation plays a more important role for the ac loss value. As an example, figure 6 shows the losses as a function of the two parameters for a transport current of 0.8I_c, computed with the 2-D model. In figure 6(a), it can be seen that the dependence of the losses on L_x becomes important only for very large values of L_z, i.e. when the electromagnetic interaction between the layers is small. For low values of L_z, the inter-layer separation L_x has practically no influence on the losses. This is confirmed in figure 6(b), where the dependence of the losses on L_z is plotted for various values of L_x. In this figure it can be

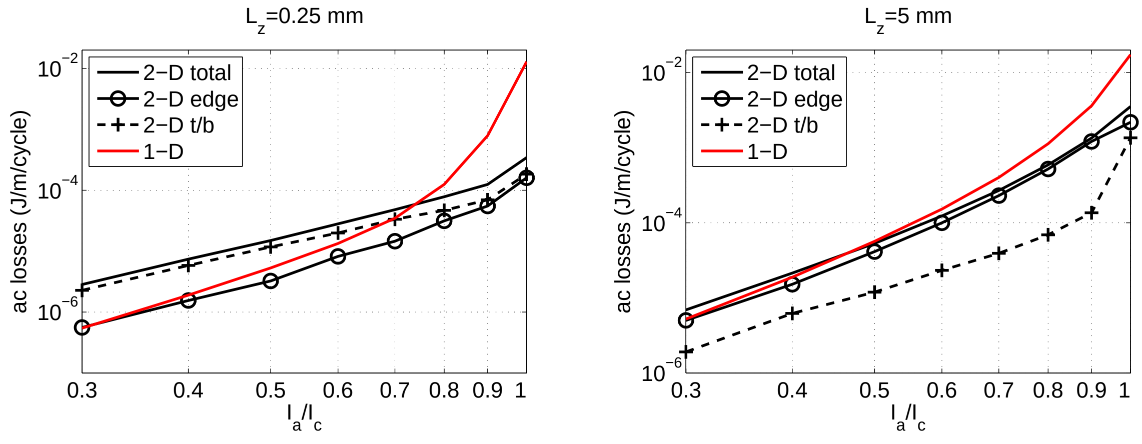

(a) (b)

Figure 5. Ac losses as a function of the transport current for L_z=0.25 mm (a) and L_z=5 mm (b), computed with the 2-D and 1-D models including the $J_c(B)$ dependence. In both cases L_x=11 mm.

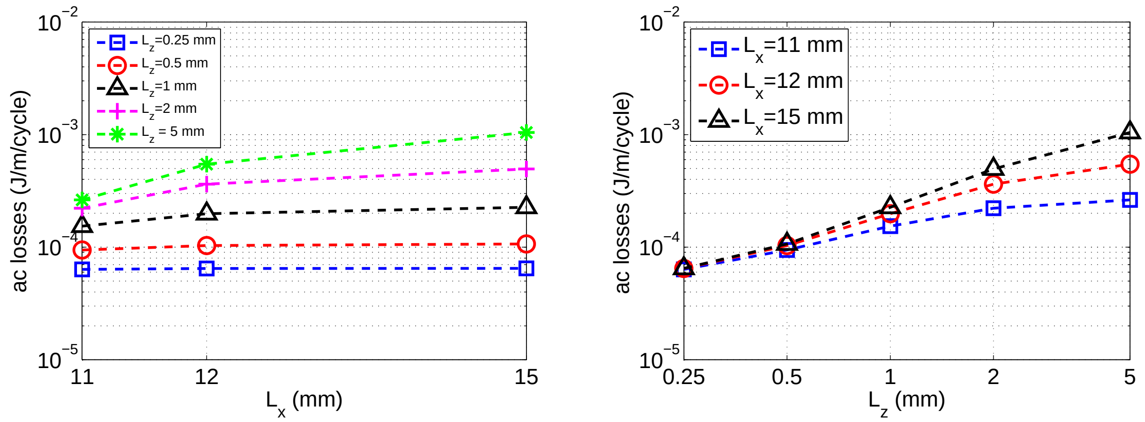

(a) (b)

Figure 6. Ac losses as a function of the size of periodic cell (a) and of the inter-layer separation (b), computed with the 2-D model for a transport current of $0.8I_c$.

noted that losses always increase with L_z, the increase being bigger for large values of L_x.

This analysis indicated that, in the design of a double non-inductive solenoid, particular care has to be taken for lowering the inter-tape distance, taking into account the manufacturing limits and the materials' constraints.

5. Conclusion

In this paper we compared two models for computing ac losses in a non-inductive solenoidal coil to be used for fault current limiter applications. In the 2-D computations, we separated the two components of the losses, i.e. the edge losses and the top/bottom losses in order to show that the 1-D model accounts only for the edge loss contribution, which outlines an important limit of the 1-D model. Indeed, while much faster than the 2-D model, the 1-D model cannot take into account the penetration of the magnetic flux from the wide faces of the superconductors, neither the associated losses. This component of the losses is particularly important when the tapes are closely packed together. On the other hand the 1-D model tends to overestimate the losses, so it can still be used for a rapid assessment of the loss level for a given configuration. Finally, we also implemented the dependence of J_c on the local magnetic field in both models. This implementation requires care in the 1-D model, in order to avoid numerical singularities arising from the computation of the magnetic field starting from the current density. We also showed that the discrepancy is between the 1-D and 2-D model is more important in the case of a field dependent J_c.

References

[1] Nguyen D N, Grilli F, Ashworth S P and Willis J O 2009 *Superconductor Science and Technology* **22** 055014
[2] Noe M and Steurer M 2007 *Superconductor Science and Technology* **20** R15–R29
[3] Kraemer H P, Schmidt W, Wohlfart M, Neumueller H W, Otto A, Verebelyi D, Schoop U and Malozemoff A P 2008 *Journal of Physics: Conference Series* **97** 012091
[4] Brambilla R, Grilli F and Martini L 2007 *Superconductor Science and Technology* **20** 16–24
[5] Brambilla R, Grilli F, Martini L and Sirois F 2008 *Superconductor Science and Technology* **21** 105008
[6] Brambilla R, Grilli F, Nguyen D N, Martini L and Sirois F 2009 *Superconductor Science and Technology* **22** 075018
[7] Sirois F, Watson D R, Zhu W and Cave J R 2002 *Proceedings of the International Cryogenic Materials Conference - ICMC* **48** 1118–1125
[8] Rostila L, Lehtonen J, Mikkonen R, Šouc J, Seiler E, Melíšek T and Vojenčiak M 2007 *Superconductor Science and Technology* **20** 1097–1100
[9] Finite-element software package Comsol Multiphysics. http://www.comsol.com
[10] Clem J R 2008 *Physical Review B* **77** 134506
[11] Nguyen D N, Ashworth S P and Willis J O 2009 *Journal of Applied Physics* **105** 063917